

A Two-Tiered Self-Powered Wireless Monitoring System Architecture for Bridge Health Management

Masahiro Kurata^a, Jerome P. Lynch^{*a,b}, Tzeno Galchev^b, Michael Flynn^b, Patrick Hipley^d,
Vince Jacob^c, Gwendolyn van der Linden^c, Amir Mortazawi^b, Khalil Najafi^b, Rebecca L. Peterson^b,
Li-Hong Sheng^d, Dennis Sylvester^b, Edward Thometz^d

^aDept. of Civil and Environmental Engineering, University of Michigan, Ann Arbor, Michigan;

^bDept. of Electrical Eng. and Computer Science, University of Michigan, Ann Arbor, Michigan;

^cSC Solutions, Inc., Sunnyvale, California;

^dCalifornia Department of Transportation, Sacramento, California

ABSTRACT

Bridges are an important societal resource used to carry vehicular traffic within a transportation network. As such, the economic impact of the failure of a bridge is high; the recent failure of the I-35W Bridge in Minnesota (2007) serves as a poignant example. Structural health monitoring (SHM) systems can be adopted to detect and quantify structural degradation and damage in an affordable and real-time manner. This paper presents a detailed overview of a multi-tiered architecture for the design of a low power wireless monitoring system for large and complex infrastructure systems. The monitoring system architecture employs two wireless sensor nodes, each with unique functional features and varying power demand. At the lowest tier of the system architecture is the ultra-low power *Phoenix* wireless sensor node whose design has been optimized to draw minimal power during standby. These ultra low-power nodes are configured to communicate their measurements to a more functionally-rich wireless sensor node residing on the second-tier of the monitoring system architecture. While the *Narada* wireless sensor node offers more memory, greater processing power and longer communication ranges, it also consumes more power during operation. Radio frequency (RF) and mechanical vibration power harvesting is integrated with the wireless sensor nodes to allow them to operate freely for long periods of time (*e.g.*, years). Elements of the proposed two-tiered monitoring system architecture are validated upon an operational long-span suspension bridge.

Keywords: wireless sensors, structural health monitoring, radio frequency power harvesting, vibration power harvesting

1. INTRODUCTION

The 2009 American Society of Civil Engineers (ASCE) report card for America's infrastructure reported that 26% of the nation's bridges are either structurally deficient or functionally obsolete [1]. The economic impact of bridge failures is quite significant given the high level of passenger and freight traffic they carry daily; the recent catastrophic failure of the I-35W Bridge (Minnesota, 2007) serves as a poignant example. In fact, the collapse (partial or total) of bridges in the United States is more frequent than what the public may think. A recent study reported that over 503 bridges of various types collapsed in the United States from 1989 to 2000 with only 13% of the cases reported in the mainstream media [2]. Although the leading cause of bridge failures are external events (*e.g.*, truck collisions, storm related floods inducing scour, traffic overload), the second predominant cause is maintenance and construction-related deficiencies.

As of December 2007, 72,524 of the nation's 599,766 bridges (12.1%) were reported as structurally deficient [3]. A bridge rated "structurally deficient" is not necessarily unsafe; rather it signifies that the bridge's deterioration must be closely monitored and that traffic (*e.g.*, volume, speed) may need to be controlled to ensure safe operation of the bridge by users. Currently, the National Bridge Inspection Program (NBIP) administered by the Federal Highway Administration (FHWA) mandates at least bi-annual inspection of every highway bridge in the United States [4]. To establish appropriate inspection procedures, bridge owners may follow technical guidelines such as the Manual for

*jerlynch@umich.edu; phone: (734) 615-5290; fax: (734) 764-4292; <http://www-personal.umich.edu/~jerlynch/>

Nondestructive Characterization for Composite Materials, Aerospace Engineering, Civil Infrastructure,
and Homeland Security 2010, edited by Peter J. Shull, Aaron A. Diaz, H. Felix Wu, Proc. of SPIE Vol. 7649
76490K · © 2010 SPIE · CCC code: 0277-786X/10/\$18 · doi: 10.1117/12.848212

Proc. of SPIE Vol. 7649 76490K-1

Bridge Evaluation (MBE) by the American Association of State Highway and Transportation Officials (AASHTO) which comprehensively highlights the key elements of an objective bridge evaluation process, *e.g.*, bridge management systems, inspection methods, load rating methods, and nondestructive load testing [5]. Recently, the need for objective information associated with bridge health management has motivated infrastructure owners to begin adopting continuous and autonomous monitoring of their assets through the use of permanent monitoring systems [6]. These structural health monitoring (SHM) systems are designed to generate quantitative measurements that empower objective evaluation of bridge conditions. This approach represents a significant improvement over the current approach of visual inspections which suffer from subjectivity introduced by inspectors.

The deployment of SHM systems to large-scale civil infrastructure systems promises to detect and track structural degradation in an affordable and real-time manner. However, the local characteristics of degradation (*e.g.*, cracking, corrosion) requires a dense network of sensors to be spatially distributed in the structure. For decades, structural monitoring systems have employed tethered communication systems. Unfortunately, the wiring demands for large infrastructure systems are high (*e.g.*, the installation of kilometers of wires) leading to expensive and time-consuming installations [7]. While wireless sensors have emerged as a possible alternative to wired sensors [8, 9, 10], the absence of long-term power sources that can offer decades of life expectancy have limited their adoption to date.

This paper presents the joint efforts of a multidisciplinary engineering team focused on the design of a new generation of wireless structural monitoring systems that can reliably operate for long periods of time without requiring continuous replacement of batteries. To achieve this goal, the team proposes the design of a two-tiered monitoring system architecture with functionality and power demand hierarchically delineated between the two tiers. Specifically, the lowest tier of the monitoring system consists of ultra-low power wireless sensor nodes that have limited functionality. Data collected by a network of these ultra-low power nodes will be wirelessly communicated over short ranges to a more powerful wireless sensor node where data is aggregated and processed. This paper presents the development of the *Phoenix* and *Narada* wireless sensor nodes for use on the lower and upper tiers of the two-tier monitoring system architecture, respectively. While power consumption has been optimized in the hardware design of both wireless sensor nodes, the development of long-term power sources is still needed. Toward this end, radio frequency (RF) and mechanical vibration power harvesting devices are designed and fabricated to provide long-term power solutions for each wireless sensor node. The paper provides an overview of the two-tiered system architecture followed by a description of field validation studies of the low-power *Narada* sensor nodes installed on the New Carquinez Bridge.

2. TWO-TIERED WIRELESS MONITORING SYSTEM ARCHITECTURE

2.1 System architecture

A multi-tier wireless monitoring system architecture is proposed for structural health monitoring of civil infrastructure systems. The system architecture is optimized to provide high sensor densities within a single structure while reducing the total power demand of the system. To achieve this goal, a two-tiered architecture is proposed herein (Fig. 1). The lower tier of the monitoring system will consist of large numbers of ultra-low power wireless sensor nodes serving as “slave” nodes to more powerful wireless sensor nodes residing on the upper tier of the architecture. The role of the wireless sensors within the upper tier is to aggregate data from the ultra-low power wireless sensors on the lower tier while also supporting in-network data processing of data and long-range communication of data to repositories within the monitoring system.

The ultra-low power wireless sensor node proposed in this study relies on three key technological innovations (Fig. 1). First, the *Phoenix* processor serves as the microprocessor core of the node. *Phoenix* is based on 0.13 μ m CMOS technology and is designed to minimize the active- and standby-mode power consumption of its digital circuit. A short-range wireless transceiver compliant with the Zigbee communication standard will be integrated with *Phoenix* for communication with wireless sensor nodes residing in the upper tier of the system architecture. The short-range Zigbee radio is designed using a custom, digital-dominant, fractional-N modulator radio circuit. The resulting sensor will enjoy a power draw of less than 20 mW which is a significant reduction in power compared to current wireless sensor nodes which currently draw 100's of mW of power.

Integrated with these impressively low-power wireless sensor nodes will be power harvesting technologies that can provide a sufficient level of sustainable power for long periods of operation. The power source must be robust in the outdoor environment with a life-expectancy on the order of decades and must not require costly maintenance (*e.g.*, battery replacement). Here, two technologies are studied for scavenging energy from bridge environments. The first is

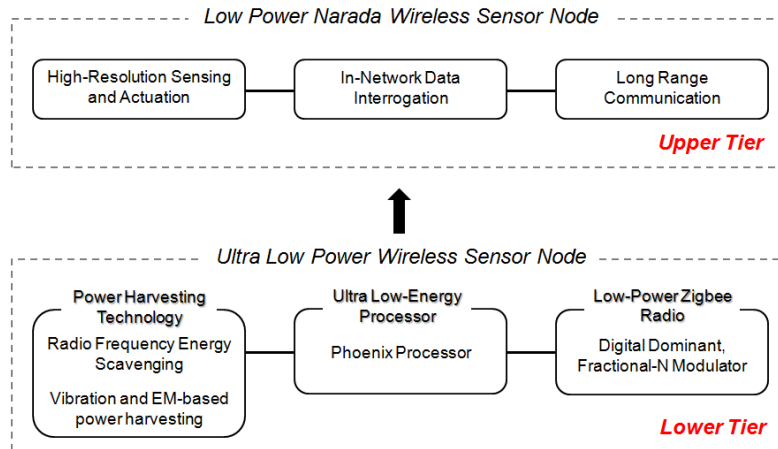


Fig. 1. Overview of the two-tiered wireless monitoring system architecture.

based on harvesting energy from the bridge's mechanical vibrations. The second power harvesting modality explored in this study is radio-frequency (RF) energy harvesting from the amplitude modulation (AM) radio spectrum.

On the upper tier of the monitoring system architecture, the *Narada* wireless sensor node is used as the primary system building block. *Narada* has been used successfully for monitoring civil infrastructure systems in the past. The *Narada* wireless sensors operate on the 2.4 GHz Zigbee radio spectrum and are capable of querying the ultra-low power wireless sensor nodes on the lower tier. While the *Narada* wireless sensor node is battery powered, the life expectancy of the node will be extended by integrating the mechanical and radio power harvesting devices with the node. Furthermore, the life expectancy of the nodes can be lengthened by minimizing the transmission of data since wireless communication consumes more power than any other device operation [9]. With computational resources (*i.e.*, a low power 8-bit microcontroller) included in the node design, sensor-based data interrogation can eliminate the need to continuously communicate raw time-history data.

2.2 Ultra Low-Power Wireless Sensor Node (Lower Tier)

2.2.1 Low Voltage Processor for Sensing Applications with a Picowatt Standby Mode

Miniaturization of sensor devices is vital in many engineering applications including implantable medical electronics, military surveillance, infrastructure monitoring, among others [11, 12]. While microelectromechanical systems (MEMS) and integrated circuit components can now meet the volume constraints for cubic millimeter sensor packages, batteries and energy scavengers cannot be easily miniaturized while providing the power demanded by the wireless sensors [13]. In this study, we explore power minimization in circuit components to further drive the power demands of sensor nodes low thereby allowing for the use of energy harvesting sources. Here, ultra-low voltage operation is achieved by minimizing active-mode power consumption in a wireless sensor's digital circuit [14, 15]. A number of well-known techniques have been widely used to reduce standby-mode power including the use of high voltage threshold (V_{th}) devices, clock gating, and power gating [16, 17].

The ultra-low power *Phoenix* processor developed at the University of Michigan is designed to leverage low voltage operation in active-mode and to draw minimal current while in standby-mode. For many typical sensing applications, the system will spend the majority of its lifetime between active measurements in standby-mode. To optimize the system for these applications, standby power should be chosen as the primary design metric with aggressive standby strategies pursued. The *Phoenix* processor consists of an 8-bit central processing unit (CPU), 52x40-bit data random access memory (RAM) also denoted as DMEM, 64x10-bit instruction RAM (denoted as IMEM), and 64x10-bit instruction read-only memory (ROM) also denoted as IROM (Fig. 2). The sensor is designed to poll a temperature sensor or strain gage, process the raw data, and store the final result in DMEM. Then the system enters standby mode between sensor measurements. The power consumption in active mode is dominated by components with high switching activity, such as the CPU. To minimize this source of power consumption, the circuit voltage is aggressively scaled to 0.5V. In standby-mode, the CPU and other inactive components are power gated. A small power gate is chosen to decrease standby power while trading off performance. The power consumed by IMEM and DMEM dominates the

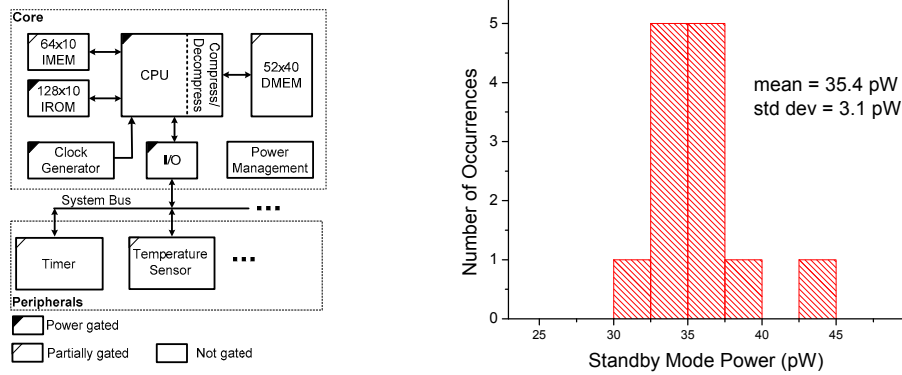


Fig. 2. (Left) the Phoenix Processor; (right) measured standby mode power distribution for 13 dies at $V_{dd} = 0.5V$.

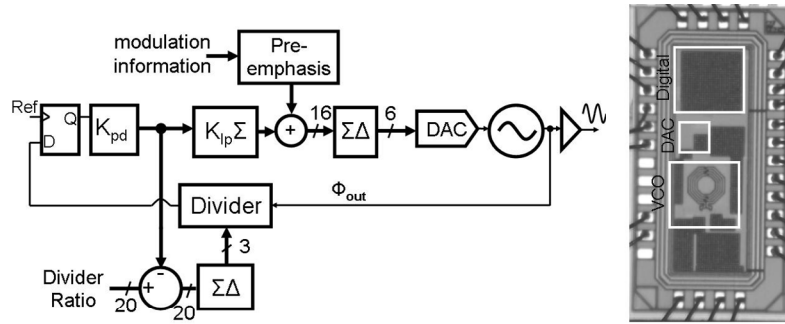


Fig. 3. (Left) fractional N modulator; (right) die photo of the working prototype [19].

processor's standby power consumption since data stored in these memory banks must be retained. To minimize standby leakage in retentive IMEM and DMEM cells, circuit techniques such as IO devices, length-biasing and device stacking are used. A test chip is fabricated in a $0.18 \mu\text{m}$ CMOS process with an area of $915 \mu\text{m}$ by $915 \mu\text{m}$. At $0.5V$, *Phoenix* operates at 106 kHz with 2.8 pJ consumed per cycle, corresponding to 297 nW . The standby-mode power is 35.4 pW with 50% of DMEM entries retained (Fig. 2). The IMEM and DMEM consume 7.1 fW/bitcell and 89% of standby power, while the power gated CPU consumes only 7% of standby power.

2.2.2 Low-Power, Digital-Dominant, Fractional-N modulator

The IEEE 802.15.4 wireless communication standard (which serves as the basis for the Zigbee wireless communication protocol) is widely used for wireless sensor networking. However, the power consumption of existing off-the-shelf wireless communication hardware typically limits battery lifetime to days or weeks. Furthermore, because several separate integrated circuits are required to make a practical sensor node, these nodes are relatively bulky. In response to these limitations, a custom, digital-dominant, fractional-N modulator architecture [18, 19] is developed for IEEE 802.15.4-compliant telemetry between the ultra-low power wireless sensor node and higher-power *Narada* sensor nodes residing on the upper tier of the monitoring system architecture. This energy efficient architecture can be integrated on the same silicon die as the *Phoenix* processor and sensor interface to achieve a chip-scale wireless sensor node. This approach enables a battery lifetime of months and makes power harvesting a viable option for battery-free operation.

The fractional-N frequency synthesizer (Fig. 3) is a key building block of wireless systems as it can both generate a high frequency signal with a well defined frequency as well as modulate that signal [20, 21]. An introduction to the use of $\Sigma\Delta$ (sigma-delta) modulation in frequency synthesis can be found in [22]. This architecture relies on a significant amount of analog circuitry. The design of analog circuits using deep sub-micron (DSM) CMOS integrated circuit technology is challenging and can often lead to excessive power dissipation, to increased sensitivity to substrate/power supply noise, and to increased sensitivity to process variation which can compromise performance or yield. Many of these problems are evident in the design of the fractional phased locked loop (PLL) elements. Charge pumps require good matching

between currents of opposite polarity. Low loop-time constants are typically required, so the loop filter must be implemented using large area capacitors or expensive off-chip components. Furthermore, these blocks do not take advantage of the major strengths of DSM technologies, which is their ability to build fast, complex, low power digital signal processing circuits.

We proposed a flexible digital-dominant fractional-N PLL modulator that improves energy efficiency and solves many of the problems associated with conventional analog fractional-N PLLs [18]. A prototype device was implemented in 0.13 μ m CMOS technology. In this scheme the phase detection technique uses a single flip-flop as a phase comparator. An additional negative feedback loop around the programmable divider keeps the phases of the two clocks aligned to within a single quantization step (Fig. 3), hence only one comparator (flip-flop) and no inverter delays are required. The die size of the prototype device is less than 1mm².

2.3 Vibration Power Harvesting

Bridges naturally vibrate under the forces of vehicular traffic and wind. This form of energy has been proposed as a possible source for harvesting power. Bridge vibrations tend to be non-periodic and low frequency, in the range of 1 to 10 Hz, with low peak amplitudes of 0.02 to 0.1 g (where 1 g = 9.8 m/s²) as shown in Fig. 4. Typical vibration harvesters use a suspended mass which moves in response to external forces. A transducer damps this motion and converts it into electrical energy. The maximum output power density scales proportionally with the input acceleration and frequency. Unfortunately, acceleration and frequency responses tend to both be low for bridges. This makes energy conversion in these environments particularly challenging. Additionally the non-periodic nature of bridge vibrations requires a wide bandwidth harvester architecture. To surmount these challenges, a broadband Parametric Frequency Increase Generator (PFIG) is newly designed [23-25]. Fig. 5 illustrates the PFIG cross-section and its behavior. The PFIG consists of a suspended mass which moves in response to the applied external force on the frame, triggering higher-frequency mechanical resonance of a frequency increased generator (FIG). Two FIGs are used: one above and one below the mass. The mass sequentially and repeatedly actuates the two FIGs by briefly latching to them using permanent NdFeB magnets. Using electromagnetic [23-25] or piezoelectric transduction [24], the FIGs convert mechanical energy into an electrical signal which can be rectified and used to power a micro-system (such as the ultra-low power wireless sensor node introduced in this study).

Three generations of PFIGs have been designed and built to date. Details of the fabrication methods and test results can be found in Galchev, *et. al.* [23-25]. The key performance metrics are summarized in Table 1. The first-generation device was a bench-top prototype which was used to demonstrate the basic PFIG architecture and to allow for ease of experimentation with the spring and magnetic latch design. This PFIG achieved a still-record average power of 39 μ W with input accelerations of 1g at 10 Hz. Note that the resonance frequency of the electro-magnetic FIG was measured to be 103 Hz, an order of magnitude greater than the external acceleration frequency, demonstrating the impressive frequency up-conversion which forms the core of the PFIG architecture.

Later PFIG generations (Table 1) have been made in self-contained modules (Fig. 6) with volumes as low as 1.2 cm³, using either electromagnetic or piezoelectric transduction. The piezoelectric FIGs typically have high resonant frequencies (975 Hz) for greater energy conversion efficiency [25]. Both the second and third generation harvesters have power densities of 2.7 μ W/cm³. All three generations break previous records of average power and power density for vibration harvesters at or below 10 Hz. Moreover, the harvesters work well for mechanical vibrations up at 20 to 24 Hz, demonstrating the broadband nature of the PFIG architecture. Work is ongoing to further improve the efficiency of the FIG transduction, improve the magnetic actuation/latching mechanism, and to design, build and test PFIGs which are optimized for the ultra-low acceleration and the low-frequency bridge vibration environment.

Table 1. Summary of non-resonant generators, measured with sinusoidal input acceleration of 1g (9.8 m/s²) at 10Hz.

Generation	Transduction mechanism	Self-contained?	Vol (cm ³)	Peak Power (μ W)	Avg. Power (μ W)	Power Density (μ W/cm ³)	Cut-off freq.
Gen 1, ¹	electro-magnetic	No	3.68*	558	39	10.7	31 Hz
Gen 2, ²	electro-magnetic	Yes	2.12	288	5.8	2.74	20 Hz
Gen 3, ³	piezoelectric	Yes	1.2	100	3.25	2.7	24 Hz

* functional volume

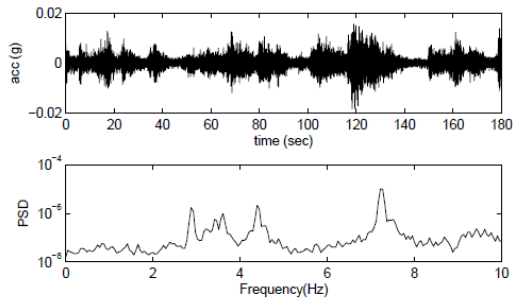


Fig. 4. Vibration of the Grove Street Bridge (Ypsilanti, Michigan): (top) acceleration; (bottom) spectral density (1st mode at 2.9 Hz).

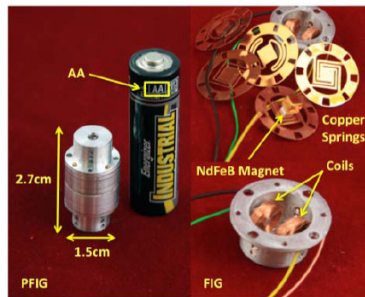


Fig. 6. (left) 2nd-generation PFIG generator assembly; (right) electromagnetic transduction FIG [25].

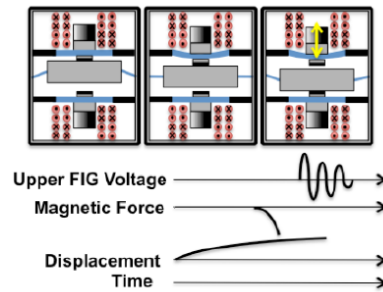
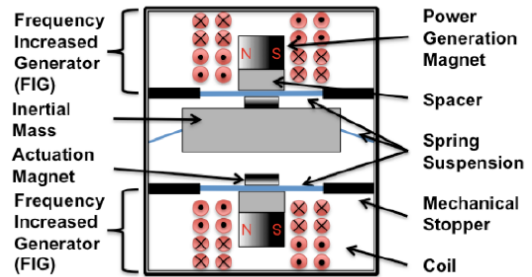


Fig. 5. Schematic of the PFIG: (top) cross-section; (bottom) kinetic behavior ([25]).

2.4 Radio Frequency Energy Scavenging

Another source for harvesting power is from the radio spectrum. Specifically, radio frequency (RF) energy scavenging circuits can be used to scavenge energy from the ambient RF broadcast spectrum. The primary challenge addressed here is the design of RF power rectifying circuits that can operate under minute input RF power levels, *i.e.* on the order of microwatts or below. Conventional rectifying circuits typically require power levels several orders of magnitude larger than the circuit used to bias the active device above its threshold voltage (V_{th}). In addition, conventional rectifying circuits require the presence of a strong RF energy source nearby the energy scavenger. The key challenges for the development of RF energy harvesters are: 1) efficient yet small antennas to pick up the stray electromagnetic signals available from radio as well as mobile phone stations; 2) efficient zero threshold rectifier circuits along with DC to DC converters and matching circuitry for proper coupling to the aforementioned antennas.

Within the radio spectrum, AM (530~1700 kHz), FM (88~108 MHz), TV (54~890 MHz) broadcast frequencies, and WiFi hotspots (2.4 / 5 GHz) are the most common ambient signals. Unfortunately, the radiation power of WiFi devices are limited to 4W as regulated by FCC requirements; these signals are also characterized by short communication ranges. In contrast, RF signals from high power broadcast stations (AM, FM and TV) are available nationwide. This availability renders broadcast stations as a promising source of energy for unattended sensor nodes deployed to the field. In this study, the AM radio spectrum is selected given its ubiquitous availability nationwide.

The block diagram of the RF scavenger proposed consists of antennas, rectifiers, charge pumps and energy storage elements (Fig. 7). Without the presence of a strong source of RF energy nearby an energy scavenger, the peak-to-peak voltage amplitude generated at the rectifier input is less than 10 mV, which is significantly lower than the typical threshold voltage for most solid state devices. Even with high-Q resonant circuits or antennas with high radiation resistances that boost the received voltage, the rectifying efficiency would still be low due to the threshold voltage drop across the solid state device. Therefore, different topologies that reduce the device threshold voltage has been explored for increasing the sensitivity of the rectifier. The most effective approach is to bias the device statically so that the effective threshold voltage can be lowered. The reverse leakage current of rectifiers is also identified as a factor which

limits the rectifier sensitivity. A cross-coupled differential configuration is adopted in order to reduce the reverse leakage current associated with rectifiers and to further improve the rectifying efficiency at low input voltage levels near the device threshold voltage.

Fig. 8 illustrates the circuit configuration that achieves an optimal rectifying performance by allowing simultaneous cancellation of the static biasing and the dynamic leakage current. In the proposed circuit, the received RF voltage is first passively amplified through the resonance formed by the inductors (L_1 and L_2) and the capacitance of the rectifier. The voltages at nodes X and Y are then charged by the NMOS transistors, M_{N1} and M_{N2} , up to a common mode voltage. Finally, the output voltage is charged by the PMOS transistors, M_{P1} and M_{P2} , to the peak voltage of node X and Y. The cross-coupled connection of the rectifier circuit allows CMOS transistors biased dynamically to lower the reverse leakage current. Floating gate capacitors C_{G1} through C_{G4} are pre-charged and connected to the gates of CMOS transistors in series, allowing static cancellation of the threshold voltages. To convert input power in the range of micro-watts into milli-watt levels, the scavenged energy will be stored continuously in a large capacitor with the circuit performance optimized for an unloaded DC output voltage. Fig. 9 shows the prototype of the proposed rectifier and a small ferrite loop stick AM antenna with a radiation efficiency of $9.7 \times 10^{-6} \%$. The power received by this prototype was measured to be around -50 dBm for a typical AM broadcast station which was tens of kilometers away from the rectifier. The performance of the prototype at this RF input environment was compared to that of a conventional low threshold germanium diode rectifier circuit (Fig. 10).

2.5 Low-Power NARADA Wireless Sensor Node (Upper Tier)

Civil structures impose unique demands on the design of a wireless sensor engaged in monitoring. One fundamental constraint is power. Therefore, low-power nodes that can operate for long periods (*e.g.*, years) on battery sources or harvested power are desired. Civil structures also require long communication ranges on the order of hundreds of meters. Finally, the low amplitude vibrations common of many civil structures requires analog-to-digital converters with high resolutions. High resolutions ensure low voltage sensor signals remain well above the quantization error inherent to the analog-to-digital conversion process.

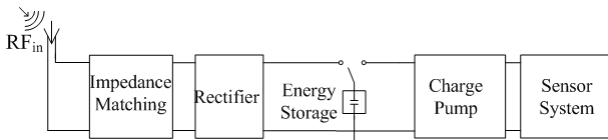


Fig. 7. Block diagram of the RF energy scavenger.

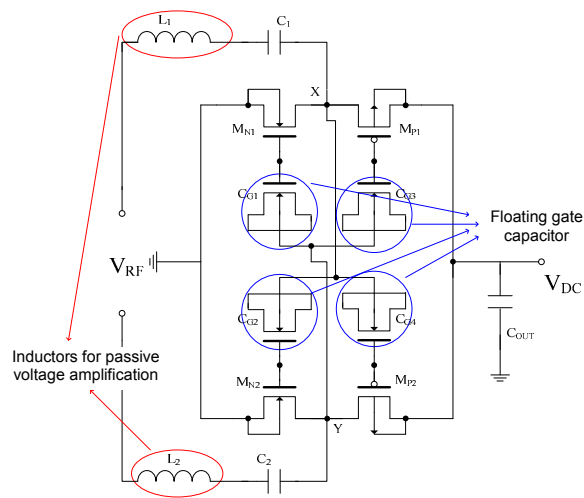
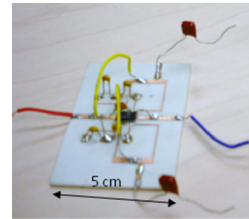


Fig. 8. Schematic of the proposed differential rectifier.

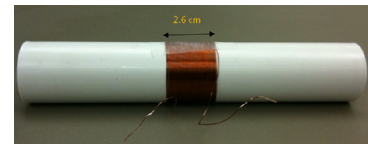


Fig. 9. (Top) proposed differential rectifier circuit; (bottom) AM ferrite antenna.

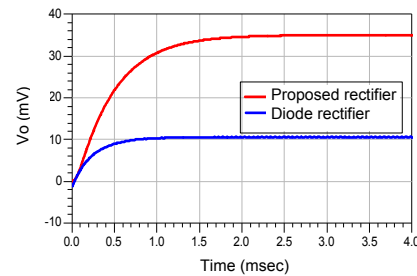


Fig. 10. Performance comparison of rectifiers.

The *Narada* wireless sensor (Fig. 11) designed at the University of Michigan [26] uses off-the-shelf embedded system components to achieve a low-power, high resolution wireless sensor that enjoys long communication ranges. The hardware design of *Narada* is decomposed into four functional blocks that support the node's capabilities to sense, communicate, compute and actuate. The first two functional blocks (*i.e.*, sensing and communication) replicate the functionality of wired sensors used in the traditional structural monitoring paradigm. The third functional block is computing; the computing available at the individual sensor node represents a significant departure from the traditional paradigm in that it empowers the wireless sensor to interrogate raw data individually or collectively with other wireless sensors in a network. In-network data processing (in lieu of communicating high-bandwidth raw data streams) has proven effective in enhancing the reliability of the wireless communication channel while preserving power in battery operated devices [27-31]. The last functional block is the actuation block. Actuation capabilities allow the wireless sensor to be engaged in control applications (for example, feedback control of structures during seismic events). The key hardware components of *Narada* are described as follows [32]:

- *Narada*'s ability to locally process data reduces demand for the communication channel; in effect, this also limits the consumption of power associated with wireless communications. Data processing takes place within the Atmel ATmega128 microcontroller which has been augmented with an additional 128 kB of external static random access memory (SRAM). The computational core also provides basic services to the sensor node such as operation of basic devices drivers, processes communication protocols, and conducts network synchronization.
- *Narada* has a four channel, high-resolution (16-bit) sensor interface (Texas Instruments ADS8341) to capture low-amplitude signals typically observed during ambient vibration testing in civil structures.
- A two-channel, 12-bit actuation interface (TI DAC7612) is provided for active sensing and control applications.
- For civil engineering structures, the short communication range (50+ m) offered by the standard CC2420 transceiver would fail to transmit distances in the hundreds of meters therefore requiring the deployment of a multi-hop wireless sensor network. However, redundant data transmissions associated with multi-hop networks consume communication bandwidth thereby limiting the effective throughput of the network as a whole [33]. To provide *Narada* with far-reaching communication ranges, a special power-amplified CC2420 transceiver circuit [Fig. 11] is fabricated for the *Narada* unit. This extended-range transceiver amplifies the CC2420 output signal by 10 dB using a power amplifier circuit between the CC2420 chip and the antenna connector. To achieve the 10 dB gain in signal, the power-amplified circuit consumes twice the current of the standard CC2420 transceiver board. Field tests of the power-amplified radio reveals that communication ranges of more than 700 m can be reliably achieved.

3. VALIDATION OF THE UPPER TIER ON A LARGE-SCALE SUSPENSION BRIDGE

3.1 System validation at the New Carquinez Bridge

The long-range communication reliability and high-resolution sensing capability of the *Narada* wireless sensor node was validated on a large-scale suspension bridge, *i.e.* the New Carquinez Bridge (NCB) in Valejo, CA. The NCB is a large

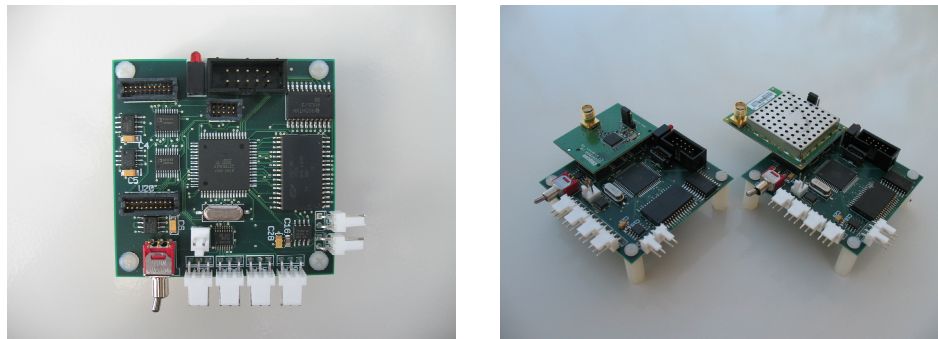


Fig. 11. *Narada* wireless sensor: (left) sensor main circuit; (right) sensor nodes with a regular and extended range IEEE802.15.4 transceiver [34].

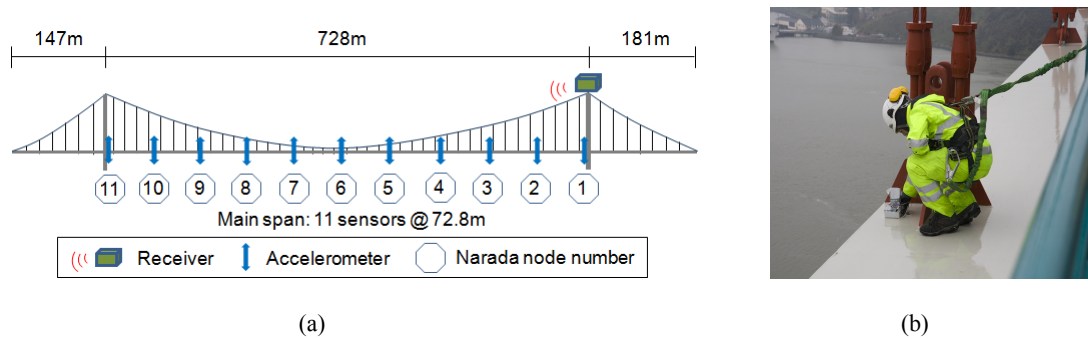


Fig. 12. *Narada* system deployment: (a) deployment plan (b) sensor node mounted on the steel surface of the bridge box.

suspension bridge with a total length of 1056m (with a main span of 728m) and consists of two anchorages, two towers, and a transition pier. The main deck is constructed from a steel orthotropic box girder while the towers consist of concrete hollow sections linked at the deck and top levels. The primary objectives of the initial field testing were to: 1) verify the scalability of a *Narada* sensor network to such a large structure; 2) collect quantitative data on the system's communication range; 3) to examine the performance of *Narada* under various weather conditions; 4) to obtain ambient vibration response data of the NCB; and 5) to identify the best suited location for permanent placement of sensors and receiver stations in future deployments.

Fig. 12(a) shows the deployment plan for the *Narada*-based wireless monitoring system installed on the NCB. The sensor nodes had MEMS accelerometers interfaced and were pre-assembled and packaged off-site in rain-proof containers. On site, the sensor packages were magnetically mounted to the surface of the steel deck outside of the bridge's walkway (see Fig. 12(b)). These sensors were verified to function correctly after 2.5 days of continuous operation with 6-AA batteries under harsh winter weather conditions (*e.g.*, heavy rain, fog, cold temperatures at night). Sensor nodes were also mounted at other locations to test the range of the radio. For example, nodes were mounted on the concrete towers, underneath the steel girder soffit, and inside the steel box girder itself.

3.2 Communication range test

When a wireless signal receiver was placed at the top of one of the towers, the *Narada* sensor nodes placed as far away as node 9 in Fig 12(a) could successfully transmit data (with a 99% success ratio) to the receiver which was approximately 700m away. However, the receiver could identify the existence of sensor node 10 but communication issues resulted in unreliable data transmission (less than a 50% success ratio). Next, *Narada* sensor nodes were magnetically attached to the underside surface of the steel box girder soffit at the location of the tower. Communication range tests were conducted using a wireless receiver located on a pneumatic inspection platform that can travel under the main deck from tower to tower. Reliable data transmission succeeded until the receiver reached a position roughly three-fourths of the span away from the tower (approximately 540m). The communication tests inside the steel box girder revealed that the RF environment was hostile to the performance of the wireless sensor. For example, internal steel diaphragms prevented the propagation of the wireless signal to distances of only 60 m. The underside of the steel box girder, which is accessible only to bridge inspectors and permitted visitors, is identified as the most promising location for the permanent installation of sensors for long-term monitoring. To capture response data from sensors installed along the underside of the deck, two receiver stations would likely be needed at each tower of the bridge.

3.3 Ambient vibration test

The ambient vibration response of the main span was measured using tri-axial accelerometers (Crossbow CXL02TG3) implemented at each of the sensor node locations in Fig. 12(a). Time histories of the vertical acceleration response acquired with a sample frequency of 100Hz for 100 seconds at sensor nodes 3 and 5 are plotted in Fig. 13. The maximum acceleration in the vertical direction exceeded 100mg at some locations under routine traffic loads. The natural frequencies of the main deck were estimated by conducting singular value decomposition of the power spectral density matrix assembled at each frequency; a plot of the first singular value as a function of frequency is presented in Fig. 14. With modal frequencies identified (Table 2), frequency domain decomposition (FDD) technique is used to extract mode shapes; FDD enables the identification of close modes with high accuracy even in the case of strong noise contamination of the signals [35, 36].

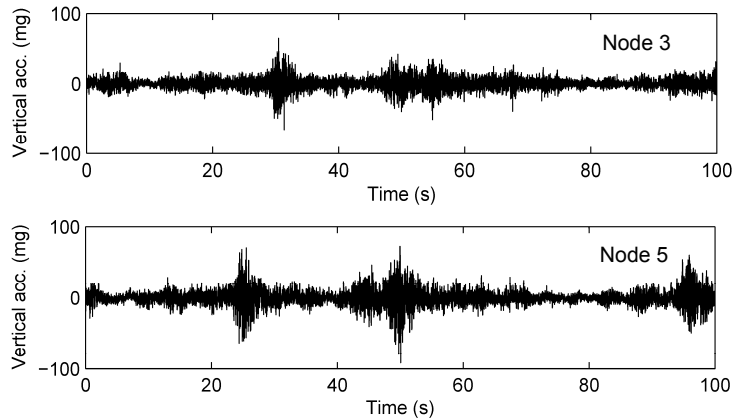


Fig 13. Vertical acceleration time histories of the main deck.

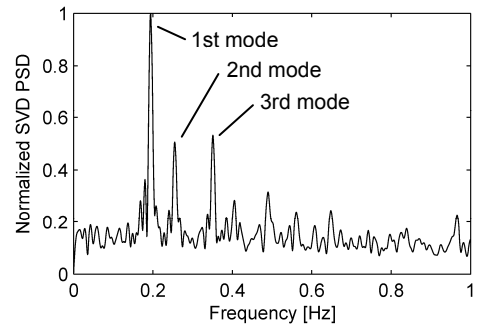


Fig 14. Singular values of response frequency function.

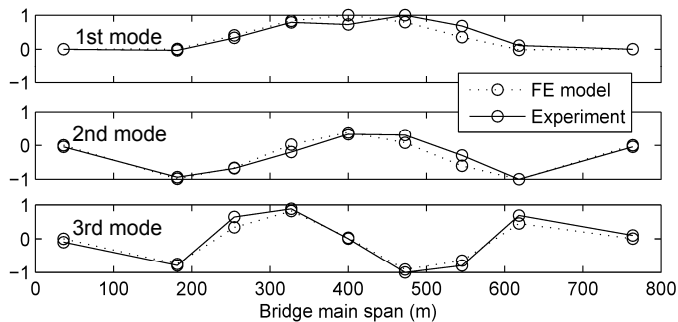


Fig 15. Vertical mode shapes of the main deck of NCB.

Table 2. Modal property comparison.

Mode	Frequency (Hz)		MAC
	Exp.	FEM	
1	0.194	0.212	0.910
2	0.255	0.271	0.929
3	0.351	0.365	0.968

The mode shapes estimated for the first three modes (0.19, 0.26, and 0.35 Hz) are plotted in Fig. 15 along with those calculated from a finite element model of the NCB. Table 2 summarizes the comparison between the experimental and numerical results; mode shapes are compared using the modal assurance criteria (MAC) as defined by Allemang and Brown [37]. It can be seen that the correlation between experiment and theory is high with MAC values exceeding 90%.

4. CONCLUSIONS

Cost-effective structural health monitoring of large-scale infrastructure systems can be advanced through the development of low-cost, but energy-efficient, wireless sensor networks. This study proposes a two-tiered wireless monitoring system architecture that utilizes different wireless sensing nodes operating on each tier. The first node is an ultra-low power node that is intended to collect strain and temperature measurements in a structure. Those measurements are then communicated using short-range radios to more powerful wireless sensor nodes that reside on the second tier of the system architecture. The more powerful nodes are designed to aggregate the data collected, process that data and to wireless communicate it over longer distances. The wireless sensor nodes on the lowest tier capitalize on four innovations. First, the ultra-low power *Phoenix* processor that adopts low active voltages and minimal standby leakage currents is explored. Second, a flexible digital-dominant fractional-N PLL modulator for short-range IEEE 802.15.4 wireless communications is proposed for the *Phoenix* processor. Third, a novel power harvesting device termed the Parametric Frequency Increase Generator (PFIG) is adopted. The PFIG utilizes a mass tuned to the dynamics of the structure to excite secondary masses that resonate at higher frequencies where energy harvesting is more efficient. Finally, a radio frequency power harvesting device is proposed to draw power from AM radio waves. On the upper tier of the system architecture, the low-power *Narada* sensor node is utilized. To validate the performance of the *Narada* wireless sensor in realistic field settings, 11 nodes were installed on the New Carquinez Bridge to record deck accelerations under ambient (*e.g.*, traffic and wind) loading conditions. The node performed well under unpleasant winter weather conditions. A wireless communication range of 700 m was validated. In addition, a large amount of bridge acceleration data was collected from which bridge mode shapes were estimated. Current efforts are focused on

the installation of a permanent wireless monitoring system within the New Carquinez Bridge. In addition, the *Phoenix*-based wireless sensor nodes are being readied for installation on the bridge for temperature measurement.

ACKNOWLEDGMENTS

The authors would like to gratefully acknowledge the generous support offered by the U.S. Department of Commerce, National Institute of Standards and Technology (NIST) Technology Innovation Program (TIP) under Cooperative Agreement Number 70NANB9H9008. Additional support was provided by the University of Michigan, Michigan Department of Transportation (MDOT), the California Department of Transportation (Caltrans), the National Science Foundation Engineering Research Center program and Sandia National Laboratory for a student fellowship.

REFERENCES

- [1] ASCE, [Report card for America's Infrastructure], American Society for Civil Engineers, <http://www.infrastructurereportcard.org/fact-sheet/bridges>, (2009).
- [2] Wardhana, K. and Hadipriono, F. C., "Analysis of recent bridge failures in the United States", *Journal of Performance of Constructed Facilities* 17 (3), 144-150 (2003).
- [3] FHWA, [Our Nation's Highways 2008], Federal Highway Administration, (2008).
- [4] Rolander, D. D., Phares, B. M., Graybeal, B. A., Moore, M. E. and Washer, G. A., "Highway bridge inspection: State-of-the-practice survey", *Transportation Research Record* 1749 (1), 73-81 (2001).
- [5] AASHTO, [Manual for Bridge Evaluation, 1st Edition], American Association of State and Highway Transportation Officials, (2008).
- [6] Lynch, J. P., Kamat, K., Li, V. C., Flynn, M. P., Sylvester, D., Najafi, K., Gordon, T., Lepech, M., Emami-Naeini, A., Krimotat, A., Ettouney, M., Alampalli, S., and Ozdemir, T., "Overview of a Cyber-enabled Wireless Monitoring System for the Protection and Management of Critical Infrastructure Systems," *SPIE Smart Structures and Materials*, San Diego, CA, (2009).
- [7] Sohn, H., Farrar, C. R., Hemez, F. M., Shunk, D. D., Stinemates, S. W., Nadler, B. R. and Czarnecki, J. J., [Review of structural health monitoring literature from 1996-2001], Los Alamos National Laboratory, Los Alamos, NM (2004).
- [8] Straser, E. and Kiremidjian, A. S., [Modular, wireless damage monitoring system for structures], John A. Blume Earthquake Engineering Center, Stanford, CA (1998).
- [9] Lynch, J. P. and Loh, K., "A summary review of wireless sensors and sensor networks for structural health monitoring", *Shock and Vibration Digest* 38(2), 91-128 (2006).
- [10] Spencer, B. F., Ruiz-Sandoval, M. E. and Kurata, N., "Smart sensing technology: Opportunities and challenges", *Journal of Structural Control and Health Monitoring* 11 (4), 349-368 (2004).
- [11] Warneke, B., Last, M., Liebowitz, B., and Pister, K., "Smart Dust: Communicating with a Cubic-Millimeter Computer," *Computer* 34(1), 44-51, 2001.
- [12] Ono, G., Nakagawa, T., Fujiwara, R., Norimatsu, T., Terada, T., Miyazaki, M., Suzuki, K., Yano, K., Ogata, Y., Maeki, A., Kobayashi, S., Koshizuka, N., and Sakamura, K., "1-cc Computer: Cross-Layer Integration with 3.4-nW/bps Link and 22-cm Locationing," *Symposium on VLSI Circuits*, 90-91 (2007).
- [13] Lin, Y.-S., Hanson, S., Albano, F., Tokunaga, C., Haque, R., Wise, K., Sastry, A., Blaauw, D., and Sylvester, D., "Low-Voltage Circuit Design for Widespread Sensing Applications," *International Symposium on Circuits and Systems*, 2558-2561 (2008).
- [14] Hanson, S., Zhai, B., Seok, M., Cline, B., Zhou, K., Singhal, M., Minuth, M., Olson, J., Nazhandali, L., Austin, T., Sylvester, D., and Blaauw, D., "Exploring Variability and Performance in a Sub-200mV Processor," *Journal of Solid-State Circuits* 43(4), 881-891 (2008).
- [15] Zhai, B., Nazhandali, L., Olson, J., Reeves, A., Minuth, M., Helfand, R., Pant, S., Blaauw, D., and Austin, T., "A 2.60pJ/Inst Subthreshold Sensor Processor for Optimal Energy Efficiency," *Symposium on VLSI Circuits*, 154-155 (2006).
- [16] Kwong, J., Ramadass, Y., Verma, N., Koesler, M., Huber, K., Moormann, H., and Chandrakasan, A., "A 65nm Sub- V_t Microcontroller with Integrated SRAM and Switched-Capacitor DC-DC Converter," *International Solid-State Circuits Conference*, 318-319 (2008).

- [17] Sheets, M., Burghardt, F., Karalar, T., Ammer, J., Chee, Y.H., and Rabaey, J., "A Power-Managed Protocol Processor for Wireless Sensor Networks," Symposium on VLSI Circuits, 212-213 (2006).
- [18] Ferriss, M. A. and Flynn, M. P., "A 14 mW Fractional-N PLL Modulator With a Digital Phase Detector and Frequency Switching Scheme," IEEE Journal of Solid-State Circuits 43(11), 2464-2471 (2008).
- [19] Ferriss, M., Lin, D., and Flynn, M. P., "A Fractional-N PLL Modulator with Flexible Direct Digital Phase Modulation," IEEE Custom Integrated Circuits Conference (CICC), (2009).
- [20] Riley, T. A., Copeland, M. A., and Kwasniewski, T. A., "Delta-sigma modulation in fractional-frequency synthesis," IEEE J. Solid-State Circuits, 28(5), 553-559, (1993).
- [21] Gotz, E., Krobek, H., Marzinger, G., Memmler, B., Munker, C., Neurauder, B., Romer, Rubach, D., J., W., Schelmbauer, Scholz, Simon, M., Steinacker, M., U., and Stoger, C., "A quad-band low power single chip direct conversion CMOS transceiver with $\Sigma\Delta$ -modulation loop for GSM," Proc. Eur. Solid-State Circuits Conf., 217-220 (2003).
- [22] Galton, I., "Delta-sigma data conversion in wireless transceivers," IEEE Trans. Theory Tech. 50(1), 302-315, (2002).
- [23] Galchev, T., Kim, H., and Najafi, K., "Non-resonant bi-stable frequency-increase power scavenger from low-frequency ambient vibration," Proceedings of the IEEE 15th International Conference on Solid-State Sensors, Actuators and Microsystems (Transducers 2009), Piscataway, NJ, USA, 632-635 (2009).
- [24] Galchev, T., Aktakka, E. E., Kim, H. and Najafi, K., "A piezoelectric frequency-increased power generator for scavenging low-frequency ambient vibration," Proceedings of the IEEE 23rd International Conference on Micro Electro Mechanical Systems (MEMS 2010), Piscataway, NJ, USA, 1203-1206 (2010).
- [25] Galchev, T., Kim, H., and Najafi, K., "A Parametric Frequency Increased Power Generator for Scavenging Low Frequency Ambient Vibrations," Proceedings of the Eurosensors XXIII Conference in Procedia Chemistry, 1(1), 1439-1442 (2009).
- [26] Swartz, A., Jung, D., Lynch, J.P., Wang, Y., Shi, D. and Flynn, M.P., "Design of a wireless sensor for scalable distributed in-network computation in a structural health monitoring system," Proceedings of 5th International Workshop on Structural Health Monitoring, Stanford, CA, (2005).
- [27] Lynch, J. P., Sundararajan, A., Law, K. H., Kiremidjian, A. S., and Carrier E., "Embedding damage detection algorithms in a wireless sensing unit for attainment of operational power efficiency," Smart Materials and Structures 13(4), 800-810 (2004).
- [28] Nagayama, T. and Spencer, B. F., [Structural Health Monitoring using Smart Sensors], NSEL Report No. NSEL-001, Department of Civil and Environmental Engineering, University of Illinois at Urbana-Champaign, IL, (2007).
- [29] Zimmerman, A. T., Shiraishi, M., Swartz, R. A., and Lynch, J. P., "Automated modal parameter estimation by parallel processing within wireless monitoring systems," ASCE Journal of Infrastructure Systems 14(1), 102-113 (2008).
- [30] Rice, J. A., Mechitov, K. A., Spencer, B. F., and Agha, G. A., "A service-oriented architecture for structural health monitoring using smart sensors," Proceedings of the 14th World Conference on Earthquake Engineering, Beijing, China, (2008).
- [31] Jones, J. D. and Pei, J. S., "Embedded algorithms within an FPGA to classify nonlinear single-degree-of-freedom systems," IEEE Sensor Journal 9(11), 1486-93 (2009).
- [32] Swartz, R.A. and Lynch, J.P., "Strategic network utilization in a wireless structural control system for seismically excited structures", ASCE Journal of Structural Engineering 135(5), 597-608 (2009).
- [33] Raghavendra, C.S., Sivalingam, K.M. and Znati, T.F., [Wireless sensor networks], Springer, New York, NY, (2004).
- [34] Kim, J., Swartz, R. A., Lynch, J. P., Lee, C. G., and Yun. C. B., "Rapid-to-Deploy Reconfigurable Wireless Structural Monitoring Systems using Extended-Range Wireless Sensors," to appear in Smart Structures and Systems, Techno Press, (2010).
- [35] Brincker, R., Zhang, L., and Anderson, P., "Modal Identification of Output-Only Systems using Frequency Domain Decomposition," Smart Mater. Struct. 10(3), 91-105 (2001).
- [36] Zimmerman, A.T., Swartz, R.A., and Lynch, J.P., "Automated identification of modal properties in a steel bridge instrumented with a dense wireless sensor network," Bridge Maintenance, Safety, Management, Health Monitoring and Informatics, 1609-1615 (2008).
- [37] Allemang, R.J. and Brown, D.L., "A correlation coefficient for modal vector analysis," Proc. Int. Modal Analysis Conf. and Exhibit, Orlando, FL, (1982).